APPLICATION OF THE INVERSE ANALYSIS TO THE HEAT TRANSFER IN FRICTION STIR WELDING

Felipe Roman Centeno, frcenteno@yahoo.com.br
Francis Henrique Ramos França, frfranca@mecanica.ufrgs.br
Departamento de Engenharia Mecânica – Universidade Federal do Rio Grande do Sul – UFRGS
Rua Sarmento Leite, nº 425, Bairro Cidade Baixa, Cep 90050-170, Porto Alegre, RS, Brasil

Abstract. *Numerical simulations of a three-dimensional conduction heat transfer process are carried out to model the friction stir welding (FSW) of AA2195-T8 aluminum plates. A finite volume code was specifically developed to model friction stir welding, which is used together with an optimization code based on Generalized Extremal Optimization (GEO) method. Based on the temperatures artificially measured at several locations on the plate for a given instant of time during the friction stir welding process, an inverse analysis of the thermal process is conducted using the GEO algorithm. The several measurement locations are determined by means of a sensitivity study which takes into account the sensitivity of the temperatures with variations on the heat source, and on each one of the heat transfer coefficients on the bottom and top surfaces. The inverse analysis aims at determining the heat generated by friction between the tool shoulder and the workpiece as well as the unknown heat transfer coefficients. This paper demonstrates that the proposed inverse approach can be an effective way to evaluate and predict the parameters that govern the complex stir welding process.*

Keywords: *Friction stir welding, finite volume analysis, inverse analysis, numerical simulation, generalized extremal optimization.*

1. INTRODUCTION

Friction stir welding (FSW) is a relatively new, state-of-the-art solid state joining process. This metal joining technique is derived from the conventional friction welding. In a typical FSW, a rotating cylindrical pin tool is forced to plunge into the plates to be welded (i.e. workpiece) and moved along their contact line. During this operation, frictional heat that is generated by contact friction between the tool and workpiece softens the material. The plasticized material is stirred by the tool and forced to "flow" to the side and the back of the tool as the tool advances. As the temperature cools down, a solid continuous joint between the two plates is then formed. Because the highest temperature in the FSW process is lower than the melting temperature of the workpiece material, FSW yields fine microstructures, absence of cracking, low residual distortion and no loss of alloying elements, which are the main advantages of this solid phase process. Nevertheless, as in the traditional fusion welds, a softened heat affected zone and a tensile residual stress parallel to the weld are also formed.

The interest in FSW has increased significantly during the last years. The thermal modelling of this process has been a central part of the FSW research since the last 1990. Basically, there are three approaches that can be done: experimental, analytical, and numerical.

Analytical approaches were reported by Gould *et al.* (1998) and Schmidt *et al.* (2003). The first ones developed an analytical FSW model. That model was based on the Rosenthal equation and described the temperature field in a quasi-steady state on a semi-inifinite plate. The temperature field was generated by means of a moving heat source. The second work proposes an analytical expression which considers the contribution of both shoulder and pin to the heat generation during the welding process.

There are several researches related to the numerical study of FSW. It is important to mention that numerical studies are intimately related with experimental studies, since numerical codes are validated by means of experimental results. An important work was presented in Soundararajan *et al.* (2005), where the authors described the heat transfer between the workpiece and the backing plate, which is a difficult parameter to be evaluated both experimentally and numerically since it depends on the stress and the contact condutance.

Furthermore, there is a specific kind of numerical approach which is called as inverse problem. Inverse analysis make use of experimental data and numerical codes. Basically, an inverse problem can be described as the solution of a problem for which the typical outputs of the forward problem are used as inputs (temperatures in the present work), and their typical inputs are used as (unknown) outputs (heat sources and heat transfer coefficients).

An inverse problem was presented in the work of Chao *et al.* (2003), which tested different values of the heat source and of the heat transfer coefficient (between the workpiece and the backing plate) until the temperature values obtained numerically were equal to those obtained experimentally during the FSW process of aluminum AA2195 sheets. This procedure was called as "best fit". The same procedure was used in Zhu and Chao (2003), but the worpiece material considered was stainless steel 304L instead of aluminum, which turn the welding process more complex due to some material parameters such as thermal conductivity and stress strength. Another contribution on inverse analysis was presented in Vilaça *et al.* (2006), in which the relation between the mechanical power imposed by the FSW machine and its amount that is transformed into friction heat was determined. In other words, they were able to provide the thermal efficiency of the FSW process. To perform this study, the authors measured temperatures in some locations on the workpiece, which were used as inputs of the inverse analisys, together with an analytical model of the heat transfer during the welding.

The present paper considers the solution of the transient three-dimensional heat conduction equation for the friction stir welding of AA2195-T8 aluminum plate using the finite volume analysis. Based on artificial measurements of temperature at different locations on the plate, an inverse analysis is carried out based on the optimization of an objective function. This function is defined as the error between the measured temperatures and the temperatures determined from the estimated parameters, which are: the heat input by the tool into the workpiece, the heat transfer coefficient between the workpiece and the support base, and the heat transfer coefficient between the workpiece and the ambient. The optimization problem is solved with the Generalized Extremal Optimization (GEO) algorithm (Sousa *et al.*, 2003). Measurement data for the temperatures are fabricated from exact values of temperatures obtained from a numerical solution performed by a given set of parameters, which are then perturbed with noises related to a set of standard deviations.

Besides, a sensitivity study is accomplished in order to find the best positions to measure the temperatures during the welding process, since this values are used as input parameters in the inverse modelling.

An important topic in the present work is the analysis of the sensibility related to the temperature readers location. This sensibility is calculated through the temperature variation in specific points on the workpiece during the welding, caused by a variation on the heat source and heat transfer coefficients values around a mean value, in this manner the points with larger sensibility values present larger variation in the temperature when the heat source or the coefficients have some change. This evaluation of very important once the solution of the inverse problem is performed using the temperature values as inputs, and the heat source values as the main output datas. At this moment, works available in the literature do not have a precise basis of the inverse analisys of the problem, which are approached only inverse problems with one or two unknown variables. These problems with two unknown variables are treated by the "trial-and-error" method, but in the present study the inverse problem is based on an optimization analysis, a much more flexible and robust technique.

2. PROBLEM DEFINITION AND NUMERICAL ANALYSIS

The modeled process considers the welding of two thin plates of aluminum AA2195-T8 using the friction stir welding (FSW) process. Each plate has 610 mm in length, 102 mm in width and 8.13 mm in thickness. The pin tool has a shoulder diameter of 25.4 mm. The geometry of the workpiece and the pin tool in a typical FSW is shown in Fig. 1. The pin tool starts at 127 mm away from the edge, and stops after translation of 584.6 mm along the weld line. The tool rotational speed is 240 rpm, and the tool translation velocity is of 2.36 mm/s; in this manner, the total welding time is 248 s. There is a pre-heat time (dwell period) of 5 seconds, in which the tool stands still at a distance of 12.7 mm from the border before it begins the translation.

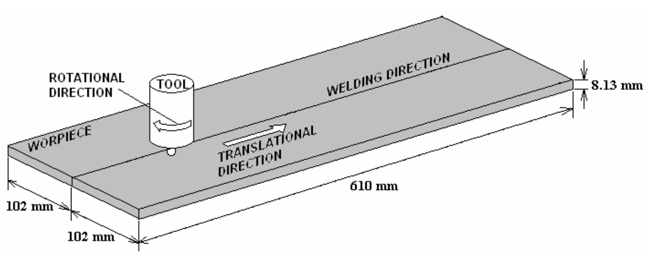

Figure 1. Geometry configuration of *FSW*

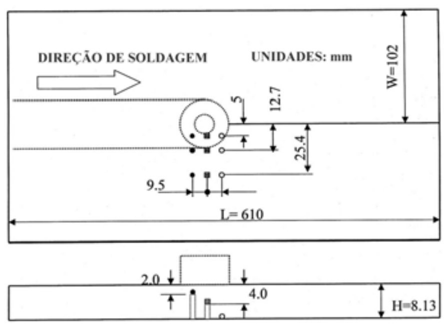

Figure 2. Locations of the temperature measurement

2.1. Finite volume method for transient heat transfer modelling

The transient temperature distribution T on the plate depends on the time t and the spatial coordinates (x, y, z), and is determined by the solution of the three-dimensional diffusion equation:

$$\rho c \frac{\partial T}{\partial t} = \frac{\partial}{\partial x}\left(k \frac{\partial T}{\partial x}\right) + \frac{\partial}{\partial y}\left(k \frac{\partial T}{\partial y}\right) + \frac{\partial}{\partial z}\left(k \frac{\partial T}{\partial z}\right) \tag{1}$$

where k is the thermal condutivity, W/(m·K), c is the specific heat capacity, in J/(kg·K), and ρ is the specific mass of the material, in kg/m³. The friction stir welding is treated as a heat source moving along the line of the welding line. The heat produced by the friction between the pin tool shoulder and the plate is concentrated locally, and propagates into the other regions of the plates by conduction, in addition to the losses by convection on the boundaries and on the bottom surface. It is assumed that the heat flux *q"* (in W/m²) imposed by the friction is distributed at the tool shoulder following the equation below:

$$q^{"}(r) = \frac{3Qr}{2\pi R_{shoulder}^{3}} \tag{2}$$

where $R_{shoulder}$ in the shoulder radius, in m, and r is the radial coordinate in m. The heat generated at the pin of the tool is neglected because it can be considered comparatively very small, e. g. in the order 2% of the total heat (Russell and Sheercliff, 1999). As such, only the heat flux imposed by the tool shoulder is considered. The heat input Q (or, alternatively, *q"*) is unknown, its determination being one of the objectives of the present inverse analysis.

On the boundaries (surfaces) of the workpiece, convection heat transfer is responsible for heat loss to the ambient, which are given by:

$$q^{"}_{conv} = h_{conv}\left(T - T_{\infty}\right) \tag{3}$$

where T_{∞} is the environment temperature, in K, h_{conv} is the convection coefficient, in W/(m²·K). In this calculation, T_{∞} = 303 K, h_{conv}= 30 W/(m²·K) are set to describe the process. Actually, the value of h_{conv} will be treated as an unknown and will be also determined from the inverse analysis. The heat loss from the bottom surface is due to heat conduction from the workpiece and support base plate, which depends on the geometry of the base as well as of the contact thermal resistance. An accurate evaluation of this heat loss is not a simple task, but experience has shown that it can be described by a rather simple relation that is similar to that used for the convection heat transfer, that is:

$$q^{"}_{b} = h_{b}\left(T - T_{b}\right) \tag{4}$$

where h_b is the heat transfer coefficient, in W/(m²·K), between the plate and the base, and T_b is the non-perturbed temperature of the base (that is, not affected by the contact with the plate), assumed here to be at the same value of the environment and surroundings, T_b = 303 K. The simple relation for the heat loss to the base requires the knowledge of the heat transfer coefficient between the plate and the supporting base, h_b. The objective of the inverse analysis is to determine h_b, in addition to the heat input Q and the convective coefficient h_{conv}, from measurements of the temperature.

Furthermore, in the numerical simulation of the FSW for AA2195-T8, it is assumed that the two plates are welded symmetrically during and after the welding. The welding line is along the symmetry line, and thus only one-half of the welded plate is modeled and the simetry surface is considered an adiabatic boundary.

In short, the boundary conditions are as follows:

- Under the tool shoulder (moving heat source): Equation (2).
- Simetry surface: Adiabatic boundary.
- Bottom surface: Equation (4).
- All other surfaces: Equation (3).

The finite volume method (FVM) code was developed, and then validated using the results reported in Chao *et al.* (2003). It is used a mesh as shown in Fig. 3, which has 122, 40 and 10 volumes in the x, y and z directions. The mesh is non-uniform in the y-direction: it has 32 volumes in the first 30 mm in the y-direction, and the remaining width of the plate is divided into 8 volumes, which obey a tangent-hiperbolic refinement equation. Besides, the temperature values are collected at the locations shown in Fig. 2, and the following values are used in the FVM code: Q = 1740 W, T_{∞} = 298 K, T_b = 298 K, h_{conv} = 30 W/(m²·K), and h_b = 350 W/(m²·K) (the same as Chao *et al.*, 2003). The values of Q, h_{conv} and h_b will be outputs of the inverse analysis. The temperature profiles obtained with the FVM code developed in the present work present a very satisfactory comparison with the results presented in Chao *et al.* (2003).

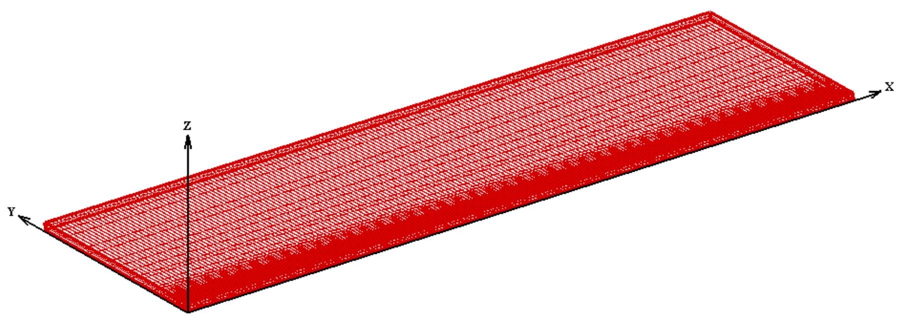

Figure 3. Finite volume method mesh.

In a grid independence study, several meshes were tested, and it was found that a mesh with 61×21×4 is refined enough to obtain good results, since using meshes more refined than this one generated nearly identical results, but the computational time increased significantly. This kind of study is very important because the FVM code will be run thousands of times during the optimization problem (inverse analysis).

The material properties of aluminum AA2195 used in the numerical solution was taken from Chao *et al.* (2003). The thermal properties are determined by the following relations (temperature T in ^{o}C):

$$k(T) = 89.643 + 0.201T \text{, [W/m·°C]} \tag{5a}$$

$$c_p(T) = 131.643 + 0.118T \text{, [J/kg·°C]} \tag{5b}$$

2.2. Sensitivity study related to the temperature acquisition locations

With the purpose of evaluating the best locations to install the temperature sensors, it was carried out a study to calculate the sensitivity of the temperature measurements for several locations on the workpiece. The role of this analysis is to indicate the best temperature measurement points, since these values are considered inputs in the inverse analysis, while the heat source and the heat transfer coefficients values are considered outputs. The points on the workpiece that present greater values of sensitivity will lead to the best results for the inverse analysis, as will be verified later in this work. S*ensitivity* is defined here as the rate in which the temperature changes with a variation in the heat source value or in the heat transfer coefficients. For instance, the sensitivity H_Q considers the temperature variation due to the variation on the heat source value, which can be expressed according to the following equation:

$$H_Q = \frac{Q}{T_{ref}} \left(\frac{\partial T}{\partial Q} \right)_i \tag{6}$$

where i represents each thermocouple (temperature sensor), Q is the heat source, in W, and T_{ref} represents a reference temperature, in K, used to make the value of H_Q dimensionless (T_{ref} = 298 K). The sensitivity H_Q can be detemined numerically by central finite differences, according to:

$$H_Q = \frac{Q}{T_{ref}} \left(\frac{T(Q+\Delta Q) - T(Q-\Delta Q)}{2\Delta Q} \right)_i \tag{7}$$

where ΔQ is the increment given to the heat source value, which was chosen to be 10% in the present work, that is, 174 W.

The two other sensitivities that were studied in this work were: the one related to the convective heat transfer coefficient, H_{hconv}; and the sensitivity related to the heat transfer coefficient at the interface between the bottom surface of the plate and the base, H_{hb}. These two sensitivities are detemined similarly to H_Q, replacing Q by h_{conv} and h_b in the Eqs. (6) and (7). The increments on h_{conv} and h_b were also chosen to correspond to 10% of their reference values.

The positions chosen to calculate these sensitivities on the workpiece are the following (the coordinate system origin is placed in the bottom surface, in the corner where the weld line starts as shown in Fig. 3):

- Direction x: 35, 85, 135, 185, 235, 285, 335, 385, 435, 485, 535 and 585 mm
- Direction y: 13, 17, 21, 25 and 29 mm
- Direction z: 0, 4.065 and 8.13 mm

In this manner, using all possible combinations of these positions led to 180 different locations that were compared based on the sensitivities of the reading of the temperature with the sought parameters: Q, h_{conv} and h_b.

Figures 4 and 5 show the results of the sensitivity H_Q for a few locations of the temperature sensors. Since the other positions presented similar trends, the results shown in Figs. 4 and 5 serve as an indication of the behavior of the sensitivities as a function of the positions of the temperature sensors.

Figure 4 shows the sensitivity H_Q variation for position x = 285 mm. In this case, the temperature measurement occurs exactly when the heat source, that is, the welding tool, is passing by this position. The figure presents the behavior of H_Q as a function of position y for three different positions z. The results for the remaining positions studied (x = 35, 85, 135, 185, 235, 335, 385, 435, 485, 535 and 585 mm) are similar to those shown in Fig. 4, which presents a decreasing in the sensitivity value with an increase in y, because the influence of the heat source decreases as the measurement points are placed farther from the welding line.

Figure 5 presents the results of the sensitivity H_Q for the temperature sensors located at y = 13 mm, for different values of x and z positions, and the data acquisition is done when the heat source (the tool) is passing by the position x = 185 mm. Again, the results for the remaining positions (17, 21, 25 and 29 mm) and for others data acquisition instants, are similar to these, showing the same behavior. The high sensitivity value, as well the remaining points, are displaced to left or right for data acquisition done when the heat source is passing by a position earlier or later than that of Fig. 5, respectively. Moreover, these results are displaced downward with an increase in y position (as verified in Fig. 4).

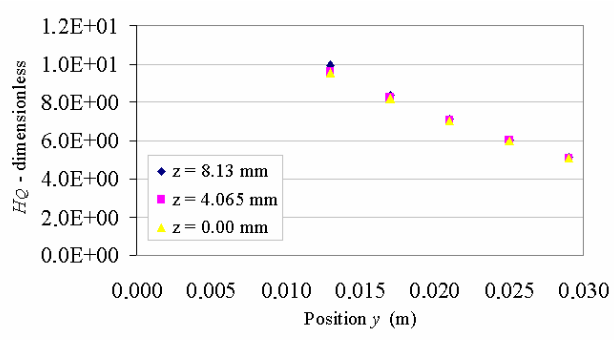

Figure 4. Sensitivity H_Q for position x = 285 mm

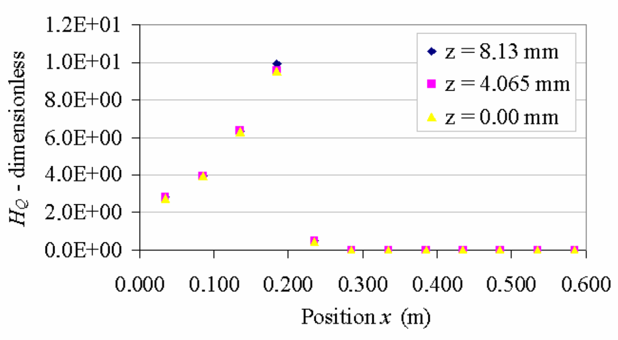

Figure 5. Sensitivity H_Q for position y = 13 mm and the heat source passing through the position x = 185 mm

At this point, all the presented results were focused on H_Q, but the sensitivities H_{hb} and H_{hconv} present a behavior that is similar to those shown in Figs. 4 and 5, except for the order of magnitude, which are much smaller than those for H_Q: $H_Q \approx 10^1$, $H_{hb} \approx 10^{-2}$ and $H_{hconv} \approx 10^{-4}$. This indicates that the temperature field is governed mainly by the heat source, being little affected by the heat transfer coefficients. In this way, the term *sensitivity* will be used from now on to describe the rate in which the temperature measurement is affected by a variation on the heat source value imposed to the workpiece, that is, the sensitivity H_Q.

Analysing the sensitivity results, several locations were selected for the collection of temperature data. These locations will be used in the inverse analysis. Besides, the effectiveness of the inverse analysis can be increased with the collection of a set of as many temperatures as it is possible, so the sensors will be gathered in eight different assemblies (three assemblies perpendicular to the weld line with ten sensors, and five assemblies parallel to the weld line with six sensors). The selected locations of the temperature sensors are presented in Tab. 1.

Table 1. Selected sensors locations based on the sensitivity results.

Sensor #	(x; y; z) in mm	Sensor #	(x; y; z) in mm	Sensor #	(x; y; z) in mm
1	(85; 13; 0)	11	(185; 13; 0)	21	(135; 13; 8.13)
2	(85; 17; 0)	12	(185; 17; 0)	22	(135; 17; 8.13)
3	(85; 21; 0)	13	(185; 21; 0)	23	(135; 21; 8.13)
4	(85; 25; 0)	14	(185; 25; 0)	24	(135; 25; 8.13)
5	(85; 29; 0)	15	(185; 29; 0)	25	(135; 29; 8.13)
6	(135; 13; 0)	16	(85; 13; 8.13)	26	(185; 13; 8.13)
7	(135; 17; 0)	17	(85; 17; 8.13)	27	(185; 17; 8.13)
8	(135; 21; 0)	18	(85; 21; 8.13)	28	(185; 21; 8.13)
9	(135; 25; 0)	19	(85; 25; 8.13)	29	(185; 25; 8.13)
10	(135; 29; 0)	20	(85; 29; 8.13)	30	(185; 29; 8.13)

The eight sensor assemblies are the folowing:
- Assembly A – Sensors 1, 2 ,3, 4, 5, 16, 17, 18, 19 and 20.
- Assembly B – Sensors 6, 7, 8, 9, 10, 21, 22, 23, 24 and 25.
- Assembly C – Sensors 11, 12, 13, 14, 15, 26, 27, 28, 29 and 30.
- Assembly D – Sensors 1, 6, 11, 16, 21 and 26.
- Assembly E – Sensors 2, 7, 12, 17, 22 and 27.
- Assembly F – Sensors 3, 8, 13, 18, 23 and 28.
- Assembly G – Sensors 4, 9, 14, 19, 24 and 29.
- Assembly H – Sensors 5, 10, 15, 20, 25 and 30.

Note that assemblies A, B and C are perpendicular to the welding line, and have ten temperature sensors, while assemblies D, E, F, G, and H are parallel to the weld line, having six temperature sensors. The acquisition data instant for assembly A occurs when the heat source is at x = 85 mm; for Assembly B, at x = 135 mm; for Assembly C, at x = 185 mm; and for Assemblies D, E, F, G and H, at x = 135 mm.

2.3. Generalized extremal optimization (GEO) method

The generalized extremal optimization (GEO) algorithm (Sousa *et al.*, 2003) is an evolutionary algorithm devised to improve the Extremal Optimization method (Boettcher and Percus, 2001) so that it could be easily applicable to virtually any kind of optimization problem. Both algorithms were inspired by the evolutionary model of Bak and Sneppen (1993). Following the Bak and Sneppen (1993) model, in GEO L species are aligned and for each species it is assigned a fitness value that will determine the species that are more prone to mutate. One can think of these species as bits that can assume the values of 0 or 1. Hence, the entire population would consist of a single binary string. The design variables of the optimization problem are encoded in this string that is similar to a chromosome in a genetic algorithm (GA) with binary representation.

To each species (bit) it is assigned a fitness number that is proportional to the gain (or loss) the objective function value has in mutating (flipping) the bit. All bits are then ranked from rank 1, for the least adapted bit, to N for the best adapted. A bit is then mutated (flipped) according to the probability distribution (1). This process is repeated until a given stopping criteria is reached and the best configuration of bits (the one that gives the best value for the objective function) found through the process is returned.

More details about this optimization method can be found in Sousa *et al.* (2003).

4. NUMERICAL EXPERIMENT - SOLUTION METHODOLOGY AND RESULTS

A simple, effective way of testing the proposed inverse analysis is to simulate the FSW process and, for given values of Q, h_b and h_{conv}, obtain the temperatures at the measurement locations shown in Tab. 1. Then, the inverse analysis is carried out to verify if the values of Q, h_b and h_{conv} can be correctly recovered. To consider a more realistic situation, for which the temperature measurements are affected by errors, the values of the temperatures obtained from the numerical simulations (for given values of Q, h_b and h_{conv}) will be perturbed by a noise according to a prescribed standard deviation σ. The objective is to evaluate how these noises can affect the estimation of Q, h_b and h_{conv}. The procedure of disturbing the numerical values of the temperatures will be denominated numerical-experimental values.

The procedure of the numerical-experiment method is outlined as follows:

1. Specify a value for the natural convection coefficient, h_{conv}. A reasonable guess is h_{conv} = 30 W/m²K;
2. Specify a value for the heat transfer coefficient at the bottom surface of the workpiece, h_b. A reasonable guess is h_b = 350 W/m²K;
3. Specify a value for the total heat input energy, Q, produced by the contact friction between the tool shoulder and the plates. A reasonable guess is Q = 1740 W;
4. Solve the three-dimensional differential equation (Eq. 1), under the previously described boundary conditions, using the finite volume numerical method. The solution of the resulting system of equations were accomplished with the TDMA method, setting a maximum relative temperature error between two subsequent iterations as 10^{-6};
5. Determine and store the thirty temperature values, T_i, for the sensors locations shown in Tab. 1;
6. Generate thirty random numbers ($rand_i$) between 0 and 1;
7. Compute: ζ_i= 0.5-$rand_i$. With the value of ζ_i select the value of η_i from a table of integrals of the gaussian normal error function;
8. Choose the value of the standard deviation (σ): 0.0% (temperature reading without noise) and 1.0% (tipical standard deviation value for infrared thermometers). It is considered that the standard deviation value associated to the temperature sensor is equal to 3σ, where σ is the standard deviation; in this manner the numerical measurement trust is of 99.73%.
9. Compute the value of the numerical-experimental temperatures: $T_i^{'} = T_i + \eta_i 3\sigma T_i$.

Steps 5 to 8 simulate measurement errors following a Gaussian distribution function with standard deviation of σ. It must be emphasized that the standard deviation values, σ, must be multiplied by T_i in the step 9 because they are present in the step 8 as percentual values, thus the value of (σT_i) on step 9 is the standard deviation value in K. In addition, the value of (σT_i) is multiplied by 3 in order to get a larger trust interval (99.73%). Table 2 shows the numercial-experimental temperatures for the thirty temperature sensors, $T_i^{'}$ (in K).

Table 2. Numerical-experimental temperature values, $T_i^{'}$ (in K).

Sensor #	3σ = 0.0%	3σ = 1.0%	Sensor #	3σ = 0.0%	3σ = 1.0%	Sensor #	3σ = 0.0%	3σ = 1.0%
1	563.235	566.281	11	567.204	570.292	21	581.744	580.293
2	517.581	519.976	12	521.759	524.196	22	526.358	527.194
3	478.153	480.388	13	482.512	484.794	23	484.287	481.690
4	445.586	444.758	14	450.081	449.232	24	450.923	453.750
5	419.029	418.898	15	423.613	423.478	25	424.046	423.533
6	566.472	569.552	16	578.540	577.105	26	582.468	581.014
7	520.988	523.417	17	522.942	523.766	27	527.131	527.970
8	481.706	483.98	18	480.710	478.157	28	485.098	482.491
9	449.248	448.403	19	447.232	450.000	29	451.764	454.604
10	422.760	422.625	20	420.283	419.783	30	424.907	424.391

5. INVERSE ANALYSIS - SOLUTION METHODOLOGY AND RESULTS

Once the numerical-experimental temperatures are obtained, the thermal-optimization analysis (inverse problem) is carried out following the steps below:

1. Specify the range of the parameters which will be optimized:
    a. Total heat generated by friction: 200 W $\leq Q \leq$ 2000 W;
    b. Heat transfer coefficient at the bottom surface: 100 W/m²K $\leq h_b \leq$ 500 W/m²K;
    c. Convective heat transfer coefficient: 10 W/m²K $\leq h_{conv} \leq$ 50 W/m²K;
2. Specify the number of function evaluations (*NFE*) at each t: *NFE = 1000*, for $1.25 \leq t \leq 2.0$ (t is changed in steps of 0.25);
3. Specify the objective function as $F(Q,h_b,h_{conv}) = \left[\sum_{i=1}^{I}\left(T_i^{'} - T_{i,cal}\right)^2\right]^{1/2}$, where $T_{i,cal}$ is the temperature computed in point *i* for given values of Q, h_{conv} and h_b, and I is equal to number of measurement points, I = 10 for assemblies A, B and C, and I = 6 for assemblies D, E, F, G and H;
4. Run GEO and obtain the value of t_{best} that return the minimum value of $F(Q,h_b,h_{conv})$ (this should provide the best estimates for Q, h_{conv} and h_b);
5. Set $t = t_{best}$ (the values of t_{best} is shown in Tab. 3 for each assembly) and enlarge *NFE (NFE* = 10000*)* for greater refinement;
6. Run GEO and obtain the final values for Q, h_{conv} and h_b.

It should be noted that the number of function evaluations (*NFE*) is equal to the number of times that the finite volum code is run for each t, which means that the finite volume code must be as efficient as possible in order to accelerate the optimization process, which is time consuming due to its evolutionary nature.

Table 3 shows the results obtained by the inverse analysis for Q_{best}, $h_{b,best}$ e $h_{conv,best}$ for the eight sensors assemblies. The table also presents the values of t_{best} for each sensor assembly. Analysing these results, it can be observed that they are in accordance with those results obtained from the sensitivity analysis presented in Section 2.2 above. Assemblies A, B and C (note that these assemblies are placed perpendicularly to the welding line) provide almost the same results, since the sensibilities for these assemblies has the same behaviour as shown in Fig. 4. For assemblies D, E, F, G and H, the results present an increase in the relative error (which ranges from 0.118% to 2.370% for Q_{best}, from 0.799% to 21.528% for $h_{b,best}$, and from 4.240% to 65.040% for $h_{conv,best}$) as the temperature sensors are placed in locations that are farther from the welding line, assembly D thru H. Note that these assemblies are placed parallel to the welding line, just increasing the distance *y* from it. Again, these results were expected since the sensitivity values decrease with the increase in the distance between the sensor location and the welding line.

Table 3. Heat source Q_{best} (W), heat transfer coefficient at bottom surface, $h_{b,best}$ (W/(m².K)), and convective heat transfer coefficient, $h_{conv,best}$ (W/(m².K)), for uncertainties of 0.0% and 1.0%.

Ass.	Uncertainty of 0.0%				Uncertainty of 1.0%			
	Q_{best} (W)	$h_{b,best}$ (W/(m².K))	$h_{conv,best}$ (W/(m².K))	t_{best}	Q_{best} (W)	$h_{b,best}$ (W/(m².K))	$h_{conv,best}$ (W/(m².K))	t_{best}
A	1769.084	409.750	14.375	1.75	1781.144	398.762	49.499	1.25
B	1769.521	410.012	12.648	2.00	1781.236	398.765	47.023	1.75
C	1765.082	311.019	41.738	1.25	1778.625	399.816	49.512	2.00
D	**1742.052**	**352.797**	**31.272**	**1.25**	**1732.628**	**355.456**	**37.631**	**1.25**
E	1742.089	354.724	31.906	1.25	1752.874	358.524	37.942	1.25
F	1745.652	365.525	21.395	1.25	1754.754	321.952	39.412	1.25
G	1717.204	319.054	42.747	1.25	1715.578	309.085	44.542	1.50
H	1718.526	312.476	48.958	1.00	1704.750	274.652	49.056	1.25

As can be observed, the sensors assembly D is the one that presents the smallest relative errors in the results for Q, h_b and h_{conv}. For uncertainty of 0.0%, the errors are of 0.118%, 0.799% and 4.240%, for Q, h_b and h_{conv}, respectively; for the case with uncertainty of 1.0%, the errors are 0.424%, 1.559% and 25.437% for the same parameters. The smallest errors in the estimation of the heat source estimation results from its greater influence on the temperature distribution on the workpiece, when compared to the influence of the heat transfer coefficients. It is emphasized that this results is in accordance with the sensitivity results shown in Section 2.2, since the sensitivity for the heat source is much larger than those for the heat transfer coefficients. Since the main objective of the present analysis is to determine the heat source in the FSW, not the heat transfer coefficients, the proposed inverse solution can be considered satisfactory.

6. CONCLUSIONS

This paper considered the estimation of parameters for the friction stir welding (FSW) of an aluminum AA2195-T8 plate. The estimation was carried out by means of an optimization problem, in which the objective function corresponded to a measure of the error between the numerically-measured temperatures and the temperatures computed for each estimated value of the heat source, and unknown heat transfer coefficients. The time-dependent temperature distribution on the plate was determined by the solution of the three-dimensional transient state diffusion equation, which was solved by the control-volume method. The minimization of the objective function was accomplished with the aid of the Generalized Extremal Optimization (GEO) algorithm, an evolutionary method that can deal with virtually any type of optimization problem. The estimation of the heat source input in the tool shoulder, the heat transfer coefficient between the plate and the base, and the convective heat transfer coefficient was carried out from the measurement of several temperatures located on the top and bottom surfaces of the plate. To simulate real-data measurements, the temperature inputs, obtained from a simulation based on specific values of the heat input and of the heat transfer coefficients were perturbed with noises according to the standard deviation of the measurement procedure. In order to obtain the best places to read the temperature values, it was done a sensitivity study. This study consisted of evaluating, in several places on the workpiece, the variations on the temperatures with variations on the sought parameters: the heat source and the heat transfer coefficients. The sensitivity for the heat source was of the order 10^1, and for the heat transfer coefficient on the base and for the convective coefficient was of the order 10^{-2} and 10^{-4}, respectively. Overall, the proposed methodology was capable of providing a satisfactory estimation for the three unknown parameters. For the heat source, the error was less than 0.5%, and for the heat transfer coefficient at the bottom surface it was less than 2.0%, while the error for the convective heat transfer coefficient reached 25.0%. The small error in the estimative of the heat source results form its greater influence on the temperature and, therefore, greater sensitivity.

As a next step in the research, it can be implemented a model which uses as inputs some mechanical characteristics desired for the welded plates, such as microstructure and hardness, since these characteristics are dependent on the temperature field. Also, this study can be extended for other welding processes, such as laser welding, where the main difference is the heat transfer in the welding region involving phase change.

7. ACKNOWLEDGEMENTS

The first author thanks CNPq for a Masters Degree scholarship. The second author thanks CNPq for research grant 304535/2007-9. Both authors thank Dr. Fabiano Luis de Sousa (INPE) for providing the GEO algorithm code.

8. REFERENCES

Bak, P. and Sneppen, K., 1993, “Punctuated Equilibrium and Criticality in a Simple Model of Evolution”, Physical Review Letters, Vol. 71, Number 24, pp. 4083-4086.

Boettcher, S. and Percus, A.G., 2001, “Optimization with Extremal Dynamics”, Physical Review Letters, Vol. 86, pp. 5211-5214.

Chao Y.J., Qi X., and Tang W., 2003, “Heat transfer in friction stir welding - experimental and numerical studies”, ASME J. Manuf. Sci. Eng. 125, pp. 138-145.

Gould J., and Feng Z., 1998, “Heat flow model for friction stir welding of aluminum alloys”, J. Mater. Process. Manuf. Sci. 7, pp. 185–194.

Russell, M. J., Sheercliff, H. R., 1999. “Analytic Modelling of Microstructure Development in Friction Stir Welding”, 1st International Symposium on Friction Stir Welding, Thousand Oaks, CA, USA.

Schmidt, H., Hattel, J., Wert, J., 2003. “An Analytical Model for the Heat Generation in Friction Stir Welding”, Modelling and Simulation in Materials Science and Engineering, vol. 12, pp. 143 – 157.

Soundararajan, V., Zekivic, S., Kovacevic, R., 2005. “Thermo-mechanical Model with Adaptive Boundary Conditions for Friction Stir Welding of Al 6061”, International Journal of Machine Tools & Manufacture, vol. 45, pp. 1577 - 1587.

Sousa, F.L., Ramos, F.M., Paglione, P., and Girardi, R. M., 2003, “New Stochastic Algorithm for Design Optimization”, AAIA Journal, Vol. 41., No. 9., pp. 1808-1818.

Vilaça, P., Quintino, L., dos Santos, J. F., Zettler, R., Sheikhi, S., 2006. “Quality Assessment of Friction Stir Welding Joints via an Analytical Thermal Model, iSTIR”, Materials Science and Engineering, vol. 445, pp. 501 – 508.

Zhu, X. K., Chao, Y. J., 2003. “Numerical Simulation of Transient Temperature ans Residual Stresses in Friction Stir Welding of 304L Stainless Steel”, Journal of Materials Processing Technology, vol. 146, pp. 263 – 272.

9. RESPONSIBILITY NOTICE